Human Brain Mapping

WILEY

RESEARCH ARTICLE OPEN ACCESS

Feasibility and Validity of Ultra-Low-Field MRI for Measurement of Regional Infant Brain Volumes in Structures Associated With Antenatal Maternal Anemia

Jessica E. Ringshaw[1,2,3] | Niall J. Bourke[3] | Michal R. Zieff[1] | Catherine J. Wedderburn[1,2] | Chiara Casella[4,5] | Layla E. Bradford[1,2] | Simone R. Williams[1,2] | Donna Herr[1] | Marlie Miles[1,2] | Jonathan O'Muircheartaigh[4,5,6] | Carly Bennallick[3] | Sean Deoni[7] | Dan J. Stein[2,8] | Daniel C. Alexander[9] | Derek K. Jones[10] | Steven C. R. Williams[3] | Kirsten A. Donald[1,2]

[1]Department of Paediatrics and Child Health, Red Cross War Memorial Children's Hospital, University of Cape Town, Cape Town, South Africa | [2]Neuroscience Institute, University of Cape Town, Cape Town, South Africa | [3]Department of Neuroimaging, Centre for Neuroimaging Sciences, Kings College London, London, England, UK | [4]Research Department of Early Life Imaging, School of Biomedical Engineering and Imaging Sciences, King's College London, London, England, UK | [5]Department for Forensic and Neurodevelopmental Sciences, Institute of Psychiatry, Psychology and Neuroscience, King's College London, London, England, UK | [6]Medical Research Council (MRC) Centre for Neurodevelopmental Disorders, King's College London, London, England, UK | [7]Maternal, Newborn, Child Nutrition and Health (MNCH) Discovery and Translational (D&T) Sciences Program, Gates Foundation, Seattle, Washington, USA | [8]South African Medical Research Council (SAMRC), Unit on Risk and Resilience in Mental Disorders, Department of Psychiatry, University of Cape Town, Cape Town, South Africa | [9]Hawkes Institute and Department of Computer Science, University College London, London, England, UK | [10]Cardiff University Brain Imaging Research Centre (CUBRIC), School of Psychology, Cardiff University, Cardiff, Wales, UK

Correspondence: Jessica E. Ringshaw (jess.ringshaw@uct.ac.za) | Kirsten A. Donald (kirsty.donald@uct.ac.za)

Received: 6 June 2025 | **Revised:** 27 October 2025 | **Accepted:** 13 December 2025

Keywords: antenatal maternal anemia | concordance | cross-validation | high-field MRI | infant brain volume | low- and middle-income countries | ultra-low-field MRI

ABSTRACT

The availability of ultra-low-field (ULF) magnetic resonance imaging (MRI) has the potential to improve neuroimaging accessibility in low-resource settings. However, the utility of ULF MRI in detecting child brain changes associated with anemia is unknown. The aim of this study was to assess the comparability of 3T high-field (HF) and 64mT ULF volumes in infants for brain regions associated with antenatal maternal anemia. This neuroimaging substudy is nested within Khula South Africa, a population-based birth cohort. Pregnant women were enrolled antenatally and postnatally, and mother–child dyads ($n = 394$) were followed prospectively at approximately 3, 6, 12, and 18 months. A subgroup of infants was scanned on 3T and 64mT MRI systems across study visits and images were segmented using MiniMORPH. Correlations and concordance coefficients were used to cross-validate HF and ULF infant brain volumes for the caudate nucleus, putamen, and corpus callosum. Seventy-eight children (53.85% male) had paired HF (mean [SD] age = 9.64 [5.26] months) and ULF (mean [SD] age = 9.47 [5.32] months) datasets. Results indicated strong agreement between systems for intracranial volume (ICV; $r = 0.96$, $\rho_{ccc} = 0.95$) and brain regions of interest in anemia including the caudate nucleus ($r = 0.89$, $\rho_{ccc} = 0.86$), putamen ($r = 0.97$, $\rho_{ccc} = 0.96$) and corpus callosum

Abbreviations: BCP, Baby Connectome Project; CSF, cerebrospinal fluid; CUBIC, Cape Universities Body Imaging Centre; DCHS, Drakenstein Child Health Study; GLHT, general linear hypothesis test; HF MRI, high-field magnetic resonance imaging; HIV, human immunodeficiency virus; ICU, intensive care unit; ICV, intracranial volume; IQT, image quality transfer; LMIC, low- and middle-income country; MOU, midwife obstetrics unit; MRI, magnetic resonance imaging; MRR, multiresolution registration; PVE, partial volume effect; QC, quality check; ROI, region of interest; SES, socioeconomic status; ULF MRI, ultra-low-field magnetic resonance imaging; UNITY, Ultra-low-field Neuroimaging In The Young; WHO, World Health Organization.

($r = 0.87$, $\rho_{ccc} = 0.79$). This cross-validation study demonstrates excellent correspondence between 3T and 64mT volumes for infant brain regions implicated in antenatal maternal anemia. Findings validate the use of ULF MRI for pediatric neuroimaging on anemia in Africa.

1 | Introduction

Anemia, a highly prevalent condition characterized by low serum hemoglobin, is a global health concern affecting approximately 571 million women (Stevens et al. 2022; WHO 2023). While all women of reproductive age are at risk of anemia, this risk is exacerbated during pregnancy when biological demands for the hemoglobin-facilitated delivery of oxygenated blood increase to support the growing fetus (Georgieff et al. 2018; Cusick and Georgieff 2016). Hemoglobin production relies on iron and is vital for the healthy maturation of the fetal brain in utero as well as the process of fetal iron loading prior to birth (Georgieff 2020). While there is a well-established association between antenatal maternal anemia and poor cognitive outcomes in children (Janbek et al. 2019; Quezada-Pinedo et al. 2021), including evidence from South Africa (Donald et al. 2019), less is known about the timing and precise underlying neurobiological mechanisms. An improved understanding of this relationship may inform the optimisation of prevention and intervention strategies for anemia in pregnancy and infancy (Wedderburn et al. 2022).

Neuroimaging tools such as magnetic resonance imaging (MRI) bridge this gap by providing a non-invasive and objective measure of assessing brain structure (Azhari et al. 2020). A few studies using high-field (HF) MRI have suggested that the developing brain may be particularly sensitive to the effects of antenatal maternal anemia (Basu et al. 2018; Loureiro et al. 2017; Monk et al. 2016). This is reinforced by findings from the Drakenstein Child Health Study (DCHS) in South Africa suggesting that these effects may be regionally consistent and tend to persist with age in children from 2–3 years (Wedderburn et al. 2022) through to age 6–7 years (Ringshaw, Hendrikse, Wedderburn, Bradford, et al. 2025). Using HF 3T MRI, maternal anemia in pregnancy was associated with 7%–8% smaller corpus callosum volumes, 5%–6% smaller caudate nucleus volumes, and 4% smaller putamen volumes in children, with remarkably comparable adjusted volume differences across timepoints. This highlights a need for corroboratory research in other high-risk settings and across timepoints, with a renewed focus on the first 2 years of life.

Conventional HF MRI systems (≥1.5 T) are expensive, requiring significant infrastructure, specialized expertise, and a high power supply (Murali et al. 2023; Anazodo et al. 2023). This technology has limited accessibility in most low- and middle-income countries (LMICs) with an average of only 0.19–1.12 MRI scanners per million people compared to high-income countries where there are approximately 26.53 MRI scanners per million people (IAEA 2025). As a result, there is disproportionately less neuroimaging research emerging from LMICs, particularly in sub-Saharan Africa, despite the burden of maternal anemia being striking in this region with 30%–50% of pregnant women estimated to be anemic (Stevens et al. 2022). In an effort to address this neuroimaging disparity, there has been an increased focus on developing scalable tools and methods that are practical for use in under-resourced settings. This includes validating the use of a novel ultra-low-field (ULF) Hyperfine Inc., Swoop 64mT MRI system (Hyperfine 2025). This mobile scanner is more cost-effective, requires less power, and is less noisy than conventional systems, allowing it to be easily integrated into low-resource settings for pediatric use (Deoni, Medeiros, et al. 2022).

Thus far, a preliminary validation study using the ULF 64mT system on neurotypical children between 6 weeks and 16 years of age in high-income settings has been positive, demonstrating strong associations between volumes extracted from structural sequences on paired HF and ULF MRI (Deoni et al. 2021). Similarly, in a study with both HF (3T) and ULF (64mT) scans, structural sequences were found to be useful for neuroanatomical identification and the detection of discrete brain abnormalities in a clinical sample of neonates in the intensive care unit (ICU) (Cawley et al. 2023). However, the utility of these systems in detecting group differences in regional brain structures associated with known risk factors of varying effect sizes for neurodevelopmental impact is unknown. Therefore, scanners have been implemented in clinical research sites across sub-Saharan Africa and South Asia as a complementary tool in ongoing research on prevalent and context-specific health priorities such as malnutrition and anemia (Abate et al. 2024).

In order to meaningfully interpret any neuroimaging findings for this important clinical research, it is necessary to determine the comparative utility of the ULF 64mT system for estimating brain volumes relative to HF MRI, with 3T typically being considered as the conventional gold standard. Cross-validation work of this nature has recently demonstrated excellent correspondence between structural outputs on 3T and 64mT MRI in healthy adults for four global tissue types and 98 local structures, with stronger concordance in larger brain regions (Váša et al. 2025). While promising, these conclusions were based on data from a sample size of 23 healthy adults. Correspondence is likely to be lower in pediatric samples due to both increased challenges acquiring data (including risks of motion artefact, poorer contrast due to incomplete myelination, and a higher water content in the developing brain) and segmenting data (segmentation inaccuracies associated with smaller absolute size of structures and the limited availability of processing pipelines with age-appropriate templates and atlases for segmentation of infant and child data) (Dagia and Ditchfield 2008; Barkovich et al. 2019; Despotović et al. 2015; Shi et al. 2010; Deoni et al. 2015). However, many of these issues are being mitigated by the implementation of clinical strategies for acquiring high-quality data by successfully scanning infants in natural sleep (Wedderburn et al. 2020), developments in ULF imaging hardware and software (Abate et al. 2024), and the optimization of

Highlights

- This cross-validation study is the first to compare high-field (HF; 3T) and ultra-low-field (ULF; 64mT) volume estimates for infant brain regions previously found to be associated with antenatal maternal anemia within the first 2 years of life.
- Key findings of this research demonstrate linear associations and strong agreement between HF and ULF volume estimates for the caudate nucleus, putamen, and corpus callosum in infants between 3 and 18 months of age. Improved correspondence between HF and ULF MRI was observed in older infants, particularly for basal ganglia structures.
- These novel findings validate the use of ULF MRI for pediatric neuroimaging work on antenatal maternal anemia and other prevalent health priorities in low- and middle-income countries (LMICs).

processing pipelines for pediatric data (Abate et al. 2024; Baljer, Zhang, et al. 2025; Baljer, Briski, et al. 2025; Casella et al. 2025). In order to assess the current feasibility of ULF MRI, similar cross-validation work needs to be conducted using paired HF and ULF data from a pediatric sample with a specific focus on brain regions affected by prevalent risk factors of interest such as anemia.

We conducted this research in infants (aged 3–18 months) who were scanned on both HF and ULF MRI scanners as part of the Khula study (Zieff et al. 2024) in South Africa. Recent epidemiological research from this cohort revealed that approximately one third of pregnant mothers were anemic and half were iron deficient after adjustment for inflammation, with 50% of antenatal anemia cases attributable to iron deficiency (Ringshaw, Zieff, Williams, et al. 2025). Given previously demonstrated HF associations between antenatal maternal anemia and smaller volumes of the corpus callosum, putamen, and caudate nucleus in toddlers (Wedderburn et al. 2022) and school-age children (Ringshaw, Hendrikse, Wedderburn, Bradford, et al. 2025), there is a need to further investigate such relationships in infants. While many other high-risk settings do not have access to paired HF and ULF MRI, the Khula study offers the opportunity to inform the feasibility of ULF MRI for research on anemia, particularly in LMICs. The aim of this study was to compare HF and ULF volume estimates for infant brain regions previously implicated with antenatal maternal anemia within the first 2 years of life.

2 | Methods

2.1 | Study Design and Setting

This neuroimaging substudy is nested within the Khula (Zieff et al. 2024) study in South Africa, an observational population-based birth cohort with a multimodal approach to investigating risk and protective factors for pediatric neurodevelopment. Mothers were recruited during the third trimester of pregnancy from antenatal clinic visits at the Gugulethu Midwife Obstetrics Unit (MOU; primary healthcare center) and in the early postnatal period from nearby clinics. Gugulethu is an urban informal settlement at sea level in the Western Cape, approximately 18 km from Cape Town, with predominantly isiXhosa speaking residents. The community is characterized by a high prevalence of psychosocial and health exposures including interpersonal violence, maternal depression, malnutrition, and infection including human immunodeficiency virus (HIV). All mother–child dyads enrolled in Khula were followed prospectively and attended study visits at approximately 3, 6, 12, and 18 months. A subgroup of infants were scanned on Siemens 3T Skyra (HF) and Hyperfine Inc., Swoop 64mT (ULF; software versions 8.2–8.6.1) systems within 90 days of each other across study visits.

2.2 | Participants

Eligibility for recruitment (December 2021—November 2022) of mothers required being over the age of 18 years and in the third trimester of pregnancy (28–36 weeks) or up to 3 months after childbirth. Exclusion criteria included multiple pregnancies, psychotropic drug use during pregnancy, infant congenital malformations or abnormalities (e.g., Spina Bifida, Down's syndrome), and severe birth complications (e.g., uterine rupture, birth asphyxia).

For the umbrella study, 394 mother–child pairs were enrolled in Khula, with 329 mothers recruited antenatally and 65 mothers recruited postnatally. Of these dyads, 246 HF scans and 535 ULF scans were collected across study visits between 3 and 18 months. All scans were subject to a rigorous visual quality check (QC) procedure performed by two senior neuroimaging staff members with training in the assessment and processing of MRI data across field strengths. This was conducted using a standardized protocol that assesses image quality based on observable indications such as motion artefact, contrast, electrical interference, signal-to-noise ratio, and field-of-view. This procedure was followed using a step-by-step form on the Flywheel platform, as per study data management protocol (Abate et al. 2024).

Any scans that failed QC were excluded from analyses, leaving 229/246 useable HF scans (93.10% success rate) and 438/535 useable ULF scans (81.87% success rate) processed on templates for age-groups 3–18 months. The predominant reason for failure across HF (94.12% [16/17] of poor-quality scans) and ULF (79.38% [77/97] of poor-quality scans) systems was motion. For both HF ($p = 0.231$) and ULF MRI ($p = 1$), there were no group differences in child sex between children whose scans passed (HF: 52.40% [120/229] boys; ULF: 52.05% [228/438] boys) versus failed (HF: 70.59% [12/17] boys; ULF: 52.58% [51/97] boys) the QC assessment. However, children whose scans failed QC (HF: mean [SD] = 4.52 [2.34] months; ULF: mean [SD] = 7.08 [4.10] months) were found to be significantly younger than children whose scans passed QC across systems (HF: mean [SD] = 11.45 [6.14] months; ULF: mean [SD] = 10.42 [5.26] months), $p < 0.001$. Overall, this data suggests that scanning success improved with age over the first 2 years of life due to improved sleep duration and decreased motion. However, it is also noted that the earlier ULF scans were acquired with older Hyperfine software contributing to poorer scan quality in younger ages.

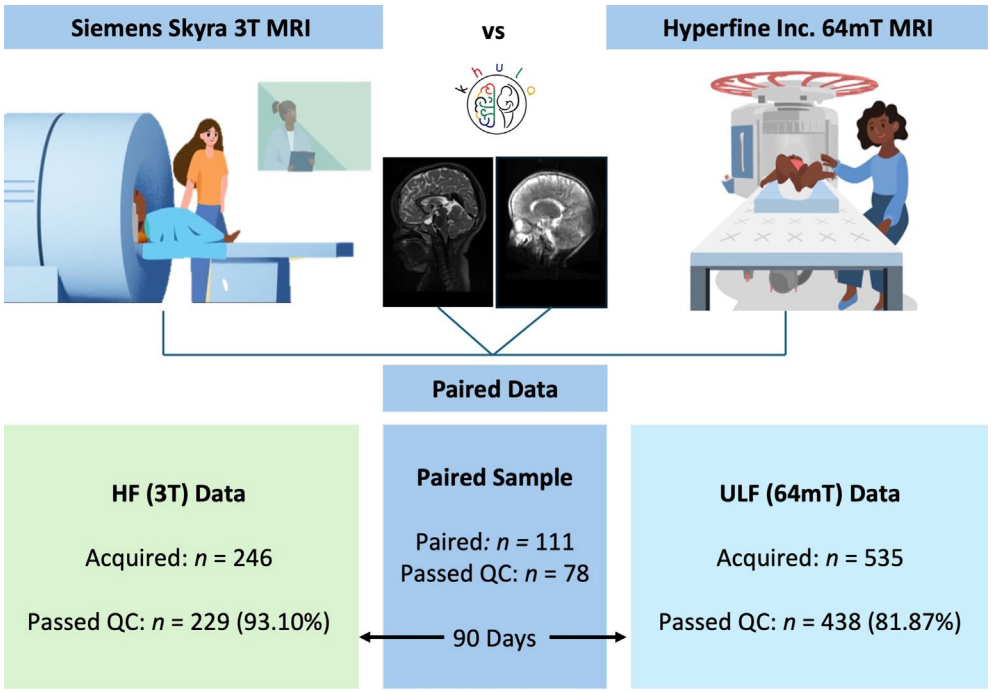

FIGURE 1 | Study flowchart demonstrating the determination of a paired sample with infant scans processed on templates for age-groups 3–18 months from HF (3T) and ULF (64mT) MRI systems. Animated images were created for neuroimaging explainer videos directed by J.E. Ringshaw as a public engagement project linked to the Khula study in South Africa. Available online for HF (Ringshaw et al. 2021a, 2021b) and ULF (Ringshaw, Wedderburn, Bradford, Williams, et al. 2025) scanning protocols.

The paired dataset ($n = 78$) was compiled for a pooled sample of infants across age groups with both useable HF and ULF scans acquired within 90 days of one another and processed with the same age template (see Section 2.3.2). The paired sample determination is illustrated in the data flowchart (Figure 1).

2.3 | Measures

2.3.1 | Demographics

Child sex and chronological age from date of birth at the time of scan were collected. Individual infant datasets (HF and ULF scans) were paired for this analysis if their age at the time of scan acquisition fell within the same age group used for template registration during processing. Additional demographic data on socioeconomic status (SES; indicated by maternal education and household income), maternal employment, and antenatal maternal anemia status was reported to provide context for the sample.

2.3.2 | Neuroimaging

2.3.2.1 | Scan Acquisition. Both HF (3T; Siemens Skyra) and ULF (64mT; Hyperfine Inc., Swoop) imaging was conducted at the Cape Universities Body Imaging Centre (CUBIC). Neuroimaging data were collected during natural sleep using strategies developed and used successfully for pediatric scanning by our team (Wedderburn et al. 2020). These include adequate preparation (desensitization, screening, rapport-building), incorporating the use of locally developed neuroimaging explainer videos for HF (Ringshaw et al. 2021a, 2021b) and ULF (Ringshaw, Wedderburn, Bradford, Williams, et al. 2025) scanning protocols, baby-friendly rooms, strategic scan timing (after other data collection activities when babies are most tired and coinciding with naps in older infants), breastfeeding (and subsequently burping to avoid discomfort due to gas) or warm meals and nappy changes prior to sleep initiation, context-specific sleep positioning (typically babies are swaddled on their mother's backs in South Africa), consistency in background noise, adequate ventilation and comfortable room temperatures, noise protection (ear plugs), immobilizing cushions for securing the head, and close body contact between research staff and babies during transfer and positioning in the scanner.

For HF MRI, T2-weighted sequences were acquired on a 3T Siemens Skyra system in the sagittal orientation using 16-channel (for infants at 3- and 6-month visits) and 32-channel (for infants at 12- and 18-month visits) head coils with the following parameters: repetition time = 3200 ms; echo time = 561 ms; voxel size $1.0 \times 1.0 \times 1.0\,mm^3$; field of view = 256 mm × 256 mm; 144 slices, 1.0 mm thick. Scan time: 3 min 30 s. ULF MRI scans were acquired on the Hyperfine Inc., Swoop 64mT system (software versions 8.2–8.6.1). Given that T2-weighted sequences are currently the most developed at ULF and best for structural imaging in infancy, they were chosen for comparative purposes. Each plane was acquired separately as orthogonal anisotropic images for axial (1.5 mm × 1.5 mm × 5 mm), coronal (1.5 mm × 5 mm × 1.5 mm), and sagittal (5 mm × 1.5 mm × 1.5 mm) sequences. All HF scans were reviewed and reported on by a clinical radiologist. Any qualitative abnormalities or incidental findings were discussed with a pediatric neurologist and, where appropriate, referred via established clinical pathways. For this study, no incidental

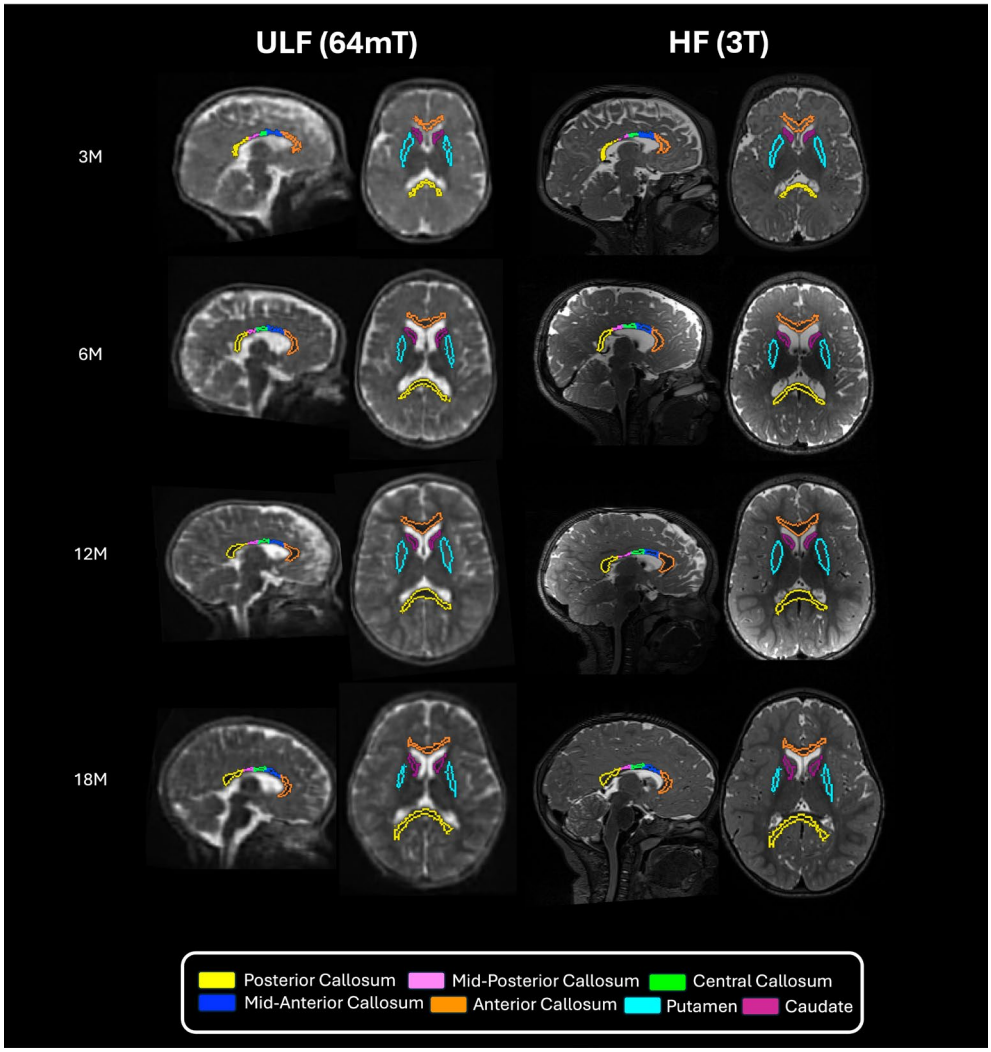

FIGURE 2 | ULF (64mT) and HF (3T) MRI data for paired subjects across age groups: examples of segmented ROIs overlaid on sagittal and axial views of T2W images.

findings were observed and therefore, no scans were excluded from the analyses on this basis.

2.3.2.2 | **Neuroimaging Processing Pipelines.** After QC of both HF and ULF raw data using the standardized protocol described above (Section 2.2), only usable scans were included in analyses. Based on previous HF findings on antenatal maternal anemia (Wedderburn et al. 2022; Ringshaw, Hendrikse, Wedderburn, Bradford, et al. 2025), volumes for the corpus callosum, caudate nucleus, and putamen were chosen as regions of interest (ROIs).

Using a multiresolution registration (MRR) technique, ULF T2W scans were reconstructed from three orthogonally acquired anisotropic images (axial, coronal, sagittal) into a single 1.5 mm^3 isotropic image of higher effective resolution (Deoni, O'Muircheartaigh, et al. 2022). Thereafter, images across field strengths (64mT and 3T) were segmented using MiniMORPH (Casella et al. 2025) (Figure 2). Tissue and cerebrospinal fluid (CSF) priors were generated by aligning Baby Connectome Project (BCP) (Chen et al. 2022) probability maps to native isotropic images via age-specific templates (Avants, Tustison, Song, et al. 2011) derived from Khula study data. Tissue priors were created by combining white matter and gray matter maps, and the skull prior was generated by dilating the brain mask for improved classification of nonbrain regions. Subcortical and callosal parcellations from BCP (Chen et al. 2022) and Penn-CHOP (Feng et al. 2019) atlases were also registered to native isotropic images (Avants, Tustison, Song, et al. 2011). Given that the Penn-CHOP atlas only includes parcellations for the total corpus callosum, the mask for this brain structure was manually divided into subregions (anterior, mid-anterior, central, mid-posterior, posterior) based on the Desikan-Killiany atlas, and reviewed for anatomical accuracy (Fischl et al. 2002). Tissue priors and masks were then registered to native T2-w isotropic images via age-specific templates (Avants, Tustison, Wu, et al. 2011). The images were segmented into the three tissue classes (tissue, CSF, and skull) using ANTs Atropos (Avants, Tustison, Wu, et al. 2011). The resulting CSF class was multiplied by the ventricle mask to separate CSF from ventricular CSF. The ANTs tissue class was multiplied by the subcortical gray matter and callosal masks to refine subcortical and callosal segmentations. The tissue class obtained from ANTs was multiplied by subcortical gray matter and callosal masks to refine subcortical and callosal segmentations.

The previously developed MRR (Deoni, O'Muircheartaigh, et al. 2022) and MiniMORPH (Casella et al. 2025) processing

pipelines were integrated to run using an automated gear implemented on Flywheel for the batch-processing of all scans. The MiniMORPH gear was set to run based on the child's age at the time of scan, using age-specific templates for 3 months (scan age < 5 months), 6 months (scan age < 10 months), 12 months (scan age < 16 months), and 18 months (scan age < 22 months).

2.4 | Statistical Analysis

Given the broad age windows of the study timepoints, individual infant datasets (HF and ULF scans) were paired based on their age at the time of scan acquisition and the corresponding age group selected for registration using Khula age-specific templates. A Z-score criterion of >3 or <-3 was used to identify outliers for regional infant brain volumes assessed separately for HF and ULF data across each respective age group. Given that no outliers were observed, no paired scans were excluded from the sample on this basis. The characteristics of the pooled sample and each age group were presented as means and standard deviations for continuous variables and frequencies for categorical variables. To test for group differences in age between scans acquired for the same children at HF and ULF, paired t tests were conducted. All statistical analyses were conducted in R Studio (2025.05.1+513) for R (Version 4.5.1) and a two-sided significance level was used throughout ($p < 0.05$).

The comparative relationship between HF and ULF MRI was assessed using Pearson's correlation coefficients (r) and Lin's concordance correlation coefficients (ρ_{ccc}) in a pooled sample of paired scans. While the correlation coefficients quantified the strength and direction of the relationship between HF and ULF volumes, the concordance coefficients demonstrated the level of agreement between HF and ULF volume estimates. This statistical analysis approach was repeated for each age group separately to assess the comparative performance and feasibility of ULF MRI in younger versus older children.

In the pooled sample with an age-specific key, the associations between HF and ULF volume estimates were graphically represented using a regression line of best fit (Figure 3). This was plotted relative to an identity line demonstrating perfect concordance (where HF and ULF are equivalent; $Y = X$) visualized as a 45° angle on axes with the same scale and dynamic range. The regression equation was used to quantify the magnitude and direction of any disagreement between HF and ULF volume estimates. Specifically, the slope (β_1) of the regression was used to assess how ULF volumes predicted HF volumes, assuming HF as the reference. Given an intercept (β_0) of 0, a slope <1 indicated systematic overestimation of HF volumes by ULF volumes (i.e., ULF values are proportionally larger than HF), while a slope >1 indicated systematic underestimation. However, in parallel, the intercept (value of Y when $X = 0$) and the crossover point (where the regression line intersects the line of identity, $Y = X$) were used to identify the value of X at which the direction of bias may switch between overestimation and underestimation. Furthermore, a general linear hypothesis test (GLHT) was used to jointly determine whether the regression model was significantly different from the line of identity ($Y = X$), as indicated by a slope that differed significantly from 1 and an intercept that differed significantly from 0. This assumed that a slope of 1 and an intercept of 0 represents perfect agreement. For brain regions with significant disagreement, the extent to which the ULF overestimated or underestimated HF regional brain volumes was quantified using percentage differences for each age group.

Finally, agreement between HF and ULF systems for ICV and regional brain volumes was explored further using Bland–Altman plots (Figure 4). The difference in HF and ULF volumes was plotted against the average brain volume measured by the two systems, with a key for age group. The mean difference line demonstrated the average bias between HF and ULF MRI, with readings closer to 0 representing stronger agreement. The limits of agreement displayed the expected range within which 95% of differences occurred, with narrow limits indicating less variability.

Given how rapidly brain growth occurs during the first 2 years of life (Knickmeyer et al. 2008; Gilmore et al. 2012), we ran sensitivity analyses to ensure that study results were not confounded by large age differences in pairings (up to a maximum of 90 days apart). These were conducted with subsamples of paired data that were compiled with shorter time intervals between HF and ULF acquisitions. Correlation and concordance coefficients were determined for paired data acquired within 60 days ($n = 72$) and 30 days ($n = 52$), respectively, and compared with the full sample of paired data acquired within 90 days ($n = 78$).

3 | Results

3.1 | Sample Characteristics

Across all study timepoints, 78 children (42 [53.85%] male) had paired HF (mean [SD] age = 9.64 [5.26] months, range = 2.56–21.07 months) and ULF (mean [SD] = 9.47 [5.32] months, range = 2.27–21.90 months) datasets. The maximum time interval between acquisitions was 90 days (observed for a single pairing), with only 7.69% (6/78) scans being more than 60 days apart. Overall, 92.31% (72/78) of scans were acquired within 60 days of each other and 66.67% (52/78) were acquired within 30 days.

In the full paired sample ($n = 78$), 52.56% (41/78) of mothers had not completed secondary school, 64.10% (50/78) of mothers were unemployed, and 66.67% (52/78) of households had a combined income of less than R5000 (approximately $300) per month. Overall, 65 mothers had antenatal maternal hemoglobin data, of which 26.15% (17/65) were found to be anemic during pregnancy. This is consistent with the broader Khula South Africa cohort (Ringshaw, Zieff, Williams, et al. 2025).

There were no differences in age between children with HF and ULF scans for paired groups overall or at 3, 6, and 18 months (Table 1). However, in the 12-month age group, children were found to be significantly older at the acquisition of their HF scan (mean [SD] = 13.60 [1.91] months) than their ULF scan (mean [SD] = 13.15 [1.76] months), $p = 0.032$.

3.2 | Cross-Validation: Full Sample

In the pooled sample with all age groups, volume estimates were significantly correlated ($p < 0.001$) with a high degree

TABLE 1 | Age distribution across HF and ULF MRI acquisitions in a paired sample ($n=78$).

Khula study Visit number	Age group in months[a]	Mean age in months *M* (SD) [range] HF (3T) MRI scan	Mean age in months *M* (SD) [range] ULF (64mT) MRI scan	*p*[b]
1	3 ($n=25$)	3.72 (0.68) [2.56–5.00]	3.58 (0.93) [2.27–4.96]	0.405
2	6 ($n=18$)	8.10 (1.37) [5.39–9.96]	7.90 (1.07) [5.39–9.60]	0.463
3	12 ($n=28$)	13.60 (1.91) [10.42–15.81]	13.15 (1.76) [9.93–15.39]	0.032*
4	18 ($n=7$)	18.94 (2.15) [16.54–21.07]	19.78 (1.79) [16.77–21.90]	0.140
Across visits	3–18 ($n=78$)	9.64 (5.26) [2.56–21.07]	9.47 (5.32) [2.27–21.90]	0.151

[a]Age groups correspond to the age-specific templates used for processing scans with MiniMORPH. The age-specific template was selected according to the infants' actual age at the time of the scan. HF and ULF MRI scans were paired if they had been processed with the same age-specific template.
[b]A paired *t* test was conducted to assess differences in age between HF MRI and ULF MRI acquisitions within the same sample.
*$p<0.05$.

of concordance for total intracranial volume (ICV; $r=0.96$, $\rho_{ccc}=0.95$), and brain ROIs in antenatal maternal anemia including the putamen ($r=0.97$, $\rho_{ccc}=0.96$), caudate nucleus ($r=0.89$, $\rho_{ccc}=0.86$), and corpus callosum ($r=0.87$, $\rho_{ccc}=0.79$). Across all age groups, the putamen emerged as having the strongest comparative relationship between HF and ULF volume estimates. Overall, Pearson's correlations and Lin's concordance coefficients were similar, demonstrating a linear relationship with strong agreement between brain volume estimates in infants between 3–18 months of age (Figure 3).

Using a joint GLHT, the linear regression model (Figure 3) for the putamen ($Y=0.94X+308.46$) did not differ significantly from the line of identity, demonstrating theoretical agreement (slope = 1) without bias (intercept = 0), $F(2,76)=2.68$, $p=0.075$. While there was strong concordance between HF and ULF volumes for the caudate nucleus, it did not represent perfect agreement as the regression line ($Y=1.07X-215.94$) differed slightly from the line of identity, $F(2,76)=3.27$, $p=0.043$. While the slope was marginally >1 suggesting systematic underestimation, the negative intercept was indicative of a downward bias and there was crossover between the regression and identity lines (Figure 3). Taken together, this model predicted that ULF overestimated HF MRI at lower brain volume ranges (younger age groups) and underestimated them at higher brain volume ranges (older age groups). The disagreement between HF and ULF MRI was more prominent for the corpus callosum ($Y=0.64X+4848.38$; $F(2,76)=62.69$, $p<0.001$) and ICV ($Y=0.83X+150905.53$; $F(2,76)=29.40$, $p<0.001$) with the regression models differing to a greater extent from the identity lines for both. In these instances, regression slopes of <1 with a positive intercept and some crossover (Figure 3) suggested ULF underestimation of HF at lower brain volumes (younger age groups) and overestimation at higher brain volumes (older age groups). The nature and magnitude of disagreement was explored further by age groups below.

3.3 | Cross-Validation: By Age Group

Cross-validation analyses were repeated for each individual age group to assess the relative predictive performance of ULF MRI in younger and older children (Table 2). These findings are discussed separately for each brain region below.

3.3.1 | ICV

Agreement between HF and ULF estimates (Table 2) for total brain volume, as indicated by ICV, strengthened with age from 3 months ($r=0.64$, $\rho_{ccc}=0.61$) to 18 months ($r=0.93$, $\rho_{ccc}=0.89$). However, there was an inconsistency at 12 months, with correlations and concordance dropping for this age group. Following on from the GLHT findings for the full sample (Figure 3), ULF underestimated HF estimates of ICV by 1.77% at 3 months, and overestimated them by 0.78% at 6 months, 4.97% at 12 months, and 3.48% at 18 months. This result was further supported by the Bland–Altman plot (Figure 4) which demonstrated a mean difference line (HF − ULF) just below 0 with slightly higher HF ICV volumes (> difference; underestimation) at 3 months and slightly lower HF volumes (< difference; overestimation) at 12 and 18 months.

3.3.2 | Basal Ganglia

The comparative association between HF and ULF volume estimates consistently improved with age for the putamen and the caudate nucleus (Table 2). By 18 months, both structures had strong positive correlations above 0.9 with similar concordance coefficients. As demonstrated using GLHT results for the full sample, HF and ULF volume estimates for the putamen were in agreement (Figures 3 and 4). Following on from the GLHT findings demonstrating marginal disagreement for the caudate nucleus in the full sample (Figure 3), ULF overestimated HF volumes for this structure by 2.60% at 3 months, and underestimated them by 3.79% at 6 months, 3.96% at 12 months, and 3.12% at 18 months. This is in alignment with the Bland–Altman plot (Figure 4), demonstrating a mean difference line (HF − ULF) just above 0, with slight overestimation (< difference) in infants at 3 months and slight underestimation (> difference) in infants at 6–18 months. However, this was marginal, with 95% of differences occurring within narrow limits of approximately $\pm 500\,mm^3$.

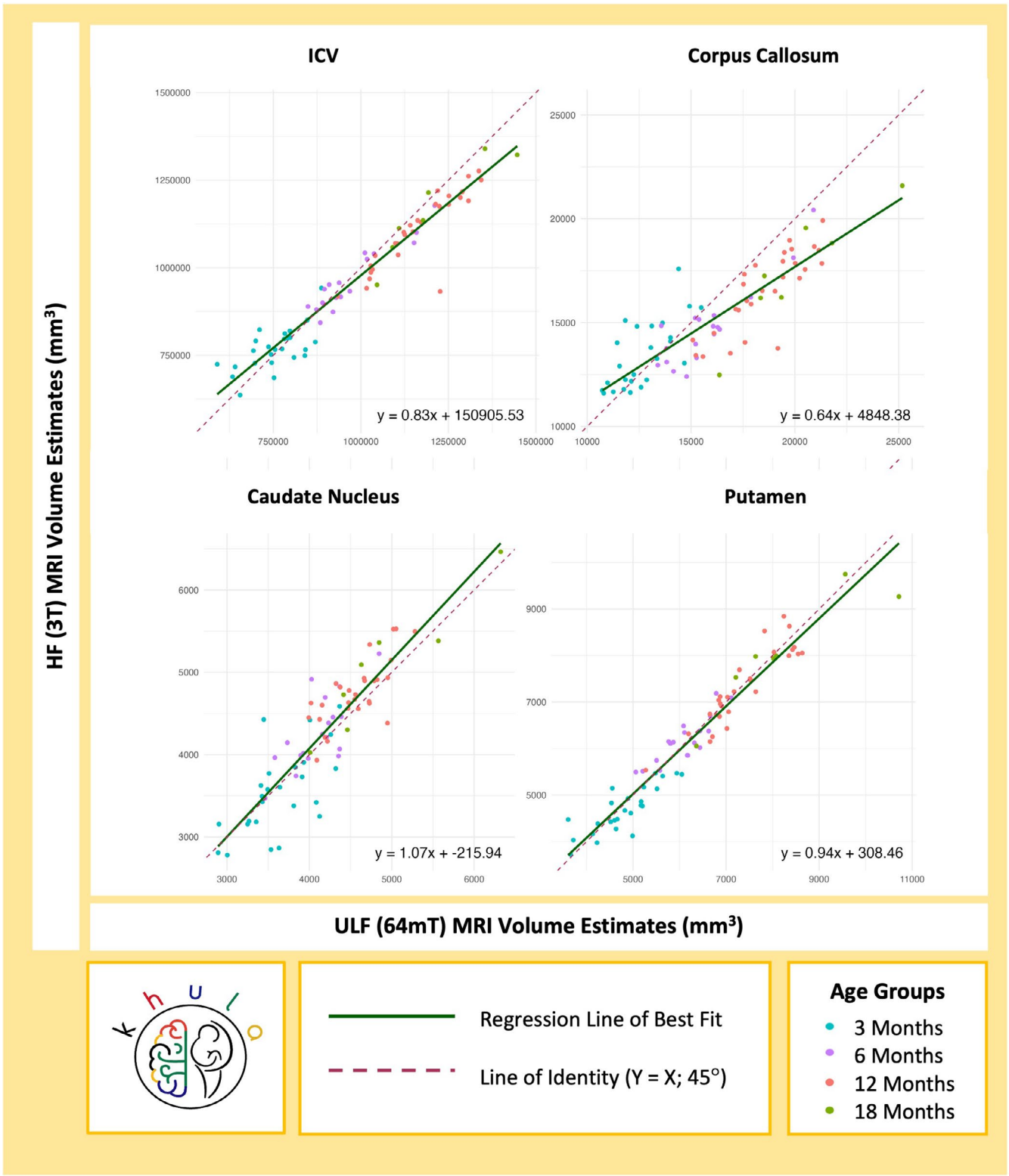

FIGURE 3 | Associations and concordance between HF (3T) and ULF (64mT) MRI volume estimates for ICV and regional brain volumes (mm^3) implicated in anemia.

3.3.3 | Corpus Callosum

There was an overall improvement (Table 2) in correlations and concordance coefficients with age for the corpus callosum from 3 months ($r = 0.69$, $\rho_{ccc} = 0.60$) to 18 months ($r = 0.92$, $\rho_{ccc} = 0.63$). However, there were inconsistencies across age groups with the strongest agreement for infants in the 6-month age group ($r = 0.90$, $\rho_{ccc} = 0.79$) followed by the weakest agreement for infants in the 12-month age group ($r = 0.82$, $\rho_{ccc} = 0.51$). Following on from the GLHT findings demonstrating disagreement and crossover in the full sample (Figure 3), it was found that the ULF system underestimated corpus callous volumes by 5.57%

TABLE 2 | Pearson's correlations and Lin's concordance coefficients for ICV and brain ROIs in antenatal maternal anemia for infants across age groups ($n = 78$).

	Correlation and concordance (r, ρ_{ccc})[a]			
Brain region	**Study visit 1: 3 months[b] ($n = 25$)**	**Study visit 2: 6 months[b] ($n = 18$)**	**Study visit 3: 12 months[b] ($n = 28$)**	**Study visit 4: 18 months[b] ($n = 7$)**
Caudate nucleus	0.63*** (0.61)	0.73*** (0.64)	0.74*** (0.65)	0.94** (0.92)
Putamen	0.83*** (0.78)	0.85*** (0.84)	0.91*** (0.91)	0.91** (0.89)
Corpus callosum	0.69*** (0.60)	0.90*** (0.79)	0.82*** (0.51)	0.92** (0.63)
ICV	0.64*** (0.61)	0.94*** (0.93)	0.88*** (0.78)	0.93** (0.89)

[a]The comparative relationship between HF and ULF MRI was assessed using Pearson's correlation coefficient (r) and Lin's concordance correlation coefficients (ρ_{ccc}) in a pooled sample of paired scans.
[b]Age groups correspond to the age-specific templates used for processing scans with MiniMORPH. The age-specific template was selected according to the infants' actual age at the time of the scan. HF and ULF MRI scans were paired if they had been processed with the same age-specific template.
**$p < 0.01$.
***$p < 0.001$.

in children at 3 months, and overestimated them by 6.77% at 6 months, 12.15% at 12 months, and 14.72% at 18 months. This was corroborated by the Bland–Altman plot (Figure 4) which revealed a pattern of differences (HF − ULF) indicative of ULF underestimating HF corpus callous volumes in younger infants at 3 months and overestimating them in older infants at 6–18 months.

Overall, the magnitude of the % volume difference between HF and ULF volumes was largest in children at 12 and 18 months, demonstrating that overestimation in older age groups occurred to a greater extent than underestimation in the younger children. This was reinforced by the Bland–Altman plot (Figure 4) with a wider lower limit (approximately—4000 mm^3) showing negative differences (overestimation) in older infants than the upper limit (approximately 2000 mm^3) showing positive differences (underestimation) in younger children.

To gain further insight into any misalignment between HF and ULF volume estimates for the corpus callosum, each segment was compared separately (Table 3). Overall, the concordance between HF and ULF volume estimates for the corpus callosum regions improved across the 3-month and 6-month age groups. However, there was less agreement in the older children, particularly in the 12-month age group. While this age-related pattern was true for all corpus callosum regions, the mid-posterior region of the corpus callosum consistently demonstrated weaker associations and lower concordance coefficients across age groups than other corpus callosum regions (Table 3).

3.4 | Sensitivity Analyses

The primary results of this study were found to be robust in sensitivity analyses, with comparable correlations and concordance coefficients between the full sample (acquired within a maximum of 90 days) and the two subsamples (acquired within a tighter window of 60 and 30 days). In comparing the paired samples with a 90-day interval relative to a 60-day interval, correlations and concordance coefficients for ICV and total regional brain volumes remained relatively unchanged, with the maximum difference being 0.02. Similarly, when comparing paired samples with a 90-day interval relative to a 30-day interval, only minor differences ranging between 0.01 (ICV, putamen, corpus callosum) and 0.05 (caudate nucleus) were observed. Given that the HF and ULF samples are not significantly different based on age (Table 1), and considering the reassuring findings in subsequent sensitivity analyses described above, the paired data in this sample was considered to be adequately matched and valid.

4 | Discussion

This study serves as the first to demonstrate the feasibility of ULF MRI for pediatric neuroimaging research on antenatal maternal anemia in LMICs, and to corroborate cross-validation work previously reported in healthy adults (Váša et al. 2025). The key finding of this research was evidence for excellent agreement between paired data across HF and ULF systems. Overall, in a pooled sample of infants between 3 and 18 months of age, there was a very strong linear relationship (Pearsons's correlations; range of $r = 0.87–0.97$) and high agreement (Lins concordance; range of $\rho = 0.79–0.96$) between 3T and 64mT brain MRI volume estimates for ICV and ROIs implicated in antenatal maternal anemia. Improved correspondence was observed in older infants, particularly, for the basal ganglia structures (caudate nucleus and putamen). While this was also true for ICV and the corpus callosum, findings were less consistent across age groups.

In assessing the overarching validity of ULF MRI for brain volume estimation across different early ages, it is likely that the basal ganglia structures were easier to segment than the corpus callosum due to their high visual contrast. The striatum of the basal ganglia (caudate nucleus and putamen) is a target of the nigrostriatal pathway with dopaminergic neurons projecting from the substantia nigra, resulting in a darker appearance on T2W MRI sequences as an indirect consequence of higher iron content (Aquino et al. 2009; Péran et al. 2009). This is

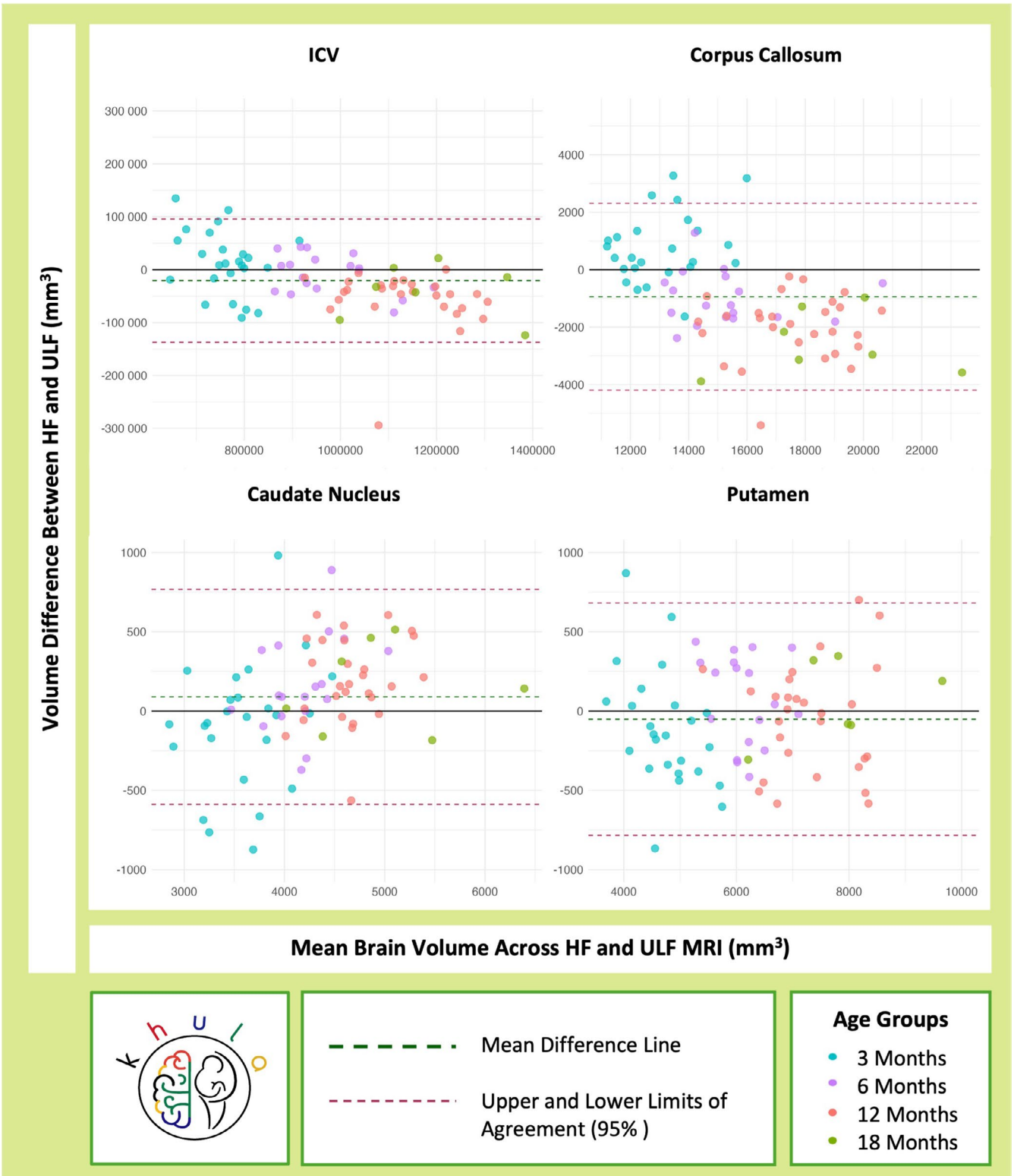

FIGURE 4 | Bland–Altman plots demonstrating the difference between HF (3T) and ULF (64mT) volume estimates for ICV and regional brain volumes implicated in anemia across age groups.

particularly prominent for the putamen, which receives the densest dopaminergic input, potentially explaining why this region emerged with the most comparable findings across HF and ULF ($r = 0.97, \rho = 0.96$) and perfect agreement between the regression model and line of identity. In contrast, the caudate nucleus has slightly less contrast than the putamen and is closer to the ventricular CSF, making it somewhat more difficult to distinguish structural boundaries for segmentation. This may have contributed to the disagreement observed for this region, although this was marginal with overestimation

TABLE 3 | Pearson's correlations and Lin's concordance coefficients for corpus callosum regions ($n = 78$).

Corpus callosum region	Correlation and concordance (r, ρ_{ccc})[a]			
	Study visit 1: 3 months [b] ($n = 25$)	Study visit 2: 6 months[b] ($n = 18$)	Study visit 3: 12 months[b] ($n = 28$)	Study visit 4: 18 months[b] ($n = 7$)
Anterior	0.69*** (0.53)	0.67** (0.60)	0.70*** (0.53)	0.95** (0.74)
Mid-anterior	0.75*** (0.60)	0.83*** (0.75)	0.68*** (0.30)	0.80* (0.49)
Central	0.77*** (0.73)	0.79*** (0.75)	0.58** (0.38)	0.78* (0.50)
Mid-posterior	0.39 (0.39)	0.74*** (0.62)	0.64*** (0.31)	0.59 (0.23)
Posterior	0.66*** (0.66)	0.93*** (0.84)	0.89*** (0.65)	0.93** (0.68)

[a]The comparative relationship between ultra low and HF MRI was assessed using Pearson's correlation coefficient (r) and Lin's concordance correlation coefficients (ρ_{ccc}) in a pooled sample of paired scans.
[b]Age groups correspond to the age-specific templates used for processing scans with MiniMORPH. The age-specific template was selected according to the infants' actual age at the time of the scan. HF and MRI scans were paired if they had been processed with the same age-specific template.
*$p < 0.05$.
**$p < 0.01$.
***$p < 0.001$.

and underestimation never exceeding 4%. While there was good correspondence across field strengths for all brain regions investigated here, the results were generally weaker for the corpus callosum with lower concordance values and a regression model that differed significantly from the line of identity. This region may have been more difficult to segment at low field strengths than the distinctive basal ganglia due to it being a narrow and intricate structure of commissural fibers connecting hemispheres, with incomplete myelination in early infancy (Barkovich and Kjos 1988; Tanaka-Arakawa et al. 2015; Deoni et al. 2011). Given its lower visual contrast on MRI, partial volume effects (PVEs), characterized by inaccuracies in voxel representation at ULF strength, may have contributed to segmentation difficulties.

Further investigation revealed general age-related patterns, with improved associations and correspondence between HF and ULF volume estimates in older infants than younger infants. This was demonstrated by a steady increase in associations and concordance from 3 months to 18 months for both the caudate nucleus ($r = 0.63$, $\rho = 0.61$ to $r = 0.94$, $\rho = 0.92$) and putamen ($r = 0.83$, $\rho = 0.78$ to $r = 0.91$, $\rho = 0.89$). This finding is to be expected in the developing brain, as ongoing myelination and maturation contribute to more discrete gray-white matter boundaries, and improved contrast for segmentation of ROIs in children over 12 months of age (Deoni et al. 2015; Croteau-Chonka et al. 2016). While this was generally true for ICV and the corpus callosum with overall improved agreement from 3 months to 18 months, there were inconsistencies across age groups. For example, concordance coefficients for ICV weakened at 12 months, with ULF 64mT volumes slightly underestimating HF estimates of ICV by 1.77% at 3 months and overestimating them by 0.78%– 4.97% in infants between 6 and 18 months. Similarly, a comparative assessment of the corpus callosum revealed the strongest agreement to be evident at 6 months ($r = 0.90$, $\rho = 0.79$) followed contrastingly by the weakest agreement at 12 months ($r = 0.82$, $\rho = 0.51$). While the ULF 64mT MRI system underestimated corpus callosum HF 3T volumes in infants at 3 months by 5.57%, the extent to which it overestimated HF corpus callosum volumes in older infants was much greater, particularly, at 12 (12.15%) and 18 (14.72%) months.

In interpreting this finding, we acknowledge that there was a group difference in age for the 12-month age group, with children being slightly older at the time of their HF 3T scan than their ULF 64mT scan. This may have biased cross-validation comparisons of total brain volume (ICV). Furthermore, given the corpus callosum's dynamic and nonlinear postnatal maturation (Tanaka-Arakawa et al. 2015), with myelination occurring in a spatiotemporal pattern (Barkovich and Kjos 1988; Deoni et al. 2011), it is possible that analyses may have been undermined by the comparison of this ROI at different stages of development. Previous research has demonstrated region-specific developmental trajectories with normal growth spurts occurring in the genu (anterior corpus callosum) at 2–3 months followed by the splenium (posterior corpus callosum) at 4–6 months (Barkovich and Kjos 1988), while postnatal myelination begins in the splenium (posterior corpus callosum) at 3–4 months and progresses rostro-caudally to the genu (anterior corpus callosum) at 6–8 months (Barkovich and Kjos 1988; Deoni et al. 2011). With such drastic changes occurring in the first year of life in opposite directions, age differences in paired data at 12 months serve as a likely explanation for generally weaker cross-validation results.

This may be exacerbated by segmentation difficulties at ULF for smaller regions of the corpus callosum body, morphologically defined by the Desikan-Killiany atlas (Fischl et al. 2002) as the mid-posterior, central, and mid-anterior corpus callosum. In particular, the mid-posterior section which corresponds with the isthmus is known to be the hardest region to segment due to interindividual variation and its narrow curved shape transitioning between the body and splenium of the corpus callosum (Cover et al. 2018). Finally, it is noted that the corpus callosum was the only structure for which the mask had to be manually divided into subregions when being created in the template space. While these were reviewed by an expert for anatomical accuracy, tracing may have introduced some error and variability contributing to less accurate

automated segmentation and generally lower concordance for this structure.

Study strengths of this research include the corroboration of established clinical strategies for successfully scanning infants in natural sleep across field strengths and the successful use of a novel template-based approach (MiniMORPH) (Casella et al. 2025) for specialized processing of pediatric MRI data. In turn, this supported the feasibility of cross-validation work in a relatively large pediatric sample. While future work would benefit from using more closely matched age groups for valid comparisons, it should also focus on improving templates to minimize any potential biases. The ongoing optimization of the MiniMORPH (Casella et al. 2025) pipeline is particularly relevant for the accurate segmentation of intricate corpus callosum regions in infant samples and is likely to be necessary for other small structures of interest such as the hippocampus. To improve generalizability of this processing method for infants, toddlers, and children, we suggest the derivation of templates from larger paired datasets across a broader age range.

ULF MRI is a rapidly growing field with ongoing advances in hardware and software. For example, continuous improvements in sequence development and software versions may further increase comparability across field strengths. Finally, for this study, correspondence was demonstrated without the prior application of synthetic enhancement using deep learning image quality transfer (IQT). While this reinforces the true validity of the findings without concern of confabulation in super-resolved images where the input does not match the training dataset (Váša et al. 2025), there is great potential for deep learning approaches to improve ULF scan quality at no additional cost (Baljer, Zhang, et al. 2025; Baljer, Briski, et al. 2025). This is an important and relevant consideration for increased scalability of neuroimaging in LMICs.

In conclusion, this study demonstrates high comparability between and HF (3T) and ULF (64mT) volumes for infant brain regions associated with antenatal maternal anemia. These novel findings represent the first paired dataset to be used to validate the use of ULF (64mT) MRI for ongoing pediatric neuroimaging work on antenatal maternal anemia across LMICs. Given that this is a relevant health priority being investigated globally, this work will be key for the meaningful interpretation of neuroimaging research findings on the impact of anemia on child brain development as well as the efficacy of ongoing interventions. This includes large-scale research projects across a collaborative international network known as ultra low-field neuroimaging in the young (UNITY) (Abate et al. 2024) in an effort to increase neuroimaging accessibility for improved maternal and child health.

Author Contributions

Jessica E. Ringshaw: conceptualization, data curation, formal analysis, funding acquisition, methodology, validation, visualization, writing – original draft. **Niall J. Bourke:** conceptualization, data curation, methodology, software, validation. **Michal R. Zieff:** conceptualization, data curation, methodology, project administration, validation. **Catherine J. Wedderburn:** conceptualization, validation. **Chiara Casella:** conceptualization, data curation, methodology, software, validation, visualization. **Layla E. Bradford:** data curation, investigation, validation. **Simone R. Williams:** investigation, validation. **Donna Herr:** project administration. **Marlie Miles:** investigation, project administration. **Jonathan O'Muircheartaigh:** conceptualization, data curation, methodology, software, validation. **Carly Bennallick:** project administration. **Khula South Africa Data Collection Team:** investigation. **Sean Deoni:** conceptualization, resources. **Dan J. Stein:** supervision, validation. **Daniel C. Alexander:** conceptualisation, methodology, validation. **Derek K. Jones:** conceptualisation, methodology, validation. **Steven C. R. Williams:** conceptualization, funding acquisition, methodology, resources, supervision, validation. **Kirsten A. Donald:** conceptualization, funding acquisition, methodology, resources, supervision, validation, writing – original draft. All authors: writing – review and editing.

Acknowledgments

We would like to thank all the mothers and infants who participated in the Khula South Africa birth cohort study and made this research possible. We are also sincerely grateful to all the staff at both the Gugulethu Midwife Obstetric Unit as well as the University of Cape Town Neuroscience Institute who were involved in recruitment and data collection. This includes the Khula South Africa Data Collection Team: Lauren Davel, Tracy Pan, Tembeka Mhlakwaphalwa, Bokang Methola, Khanyisa Nkubungu, Candice Knipe, Zamazimba Madi, Nwabisa Mlandu, Ringie Gulwa, and Pamela Madikane.

Funding

The Khula birth cohort was supported by the Wellcome Leap 1kD program (The First 1000 Days; 222076/Z/20/Z). J.E. Ringshaw is supported by a Wellcome Trust International Training Fellowship (224287/Z/21/Z). K.A. Donald was awarded funding from the Gates Foundation (INV-023509) in support of the anemia analyses. J.E. Ringshaw, C.J. Wedderburn, L.E. Bradford, S.R. Williams, M. Miles, and K.A. Donald are all supported by the DELTAS II Africa Programme (Del-22-002) which is funded by the Science for Africa Foundation with support from the Wellcome Trust and the UK Foreign, Commonwealth and Development Office and is part of the the EDCTP 2 programme supported by the European Union. S.C.R. Williams is supported by the Gates Foundation (INV-047888) and the National Institute for Health and Care Research (NIHR) Maudsley Biomedical Research Centre (BRC). D.J. Stein is supported by the South African Medical Research Council (SAMRC). The funders had no role in study design, data collection and analysis, decision to publish, or preparation of the manuscript. For the purpose of open access, the authors have applied a CC BY public copyright licence to any Author Accepted Manuscript version arising from this submission.

Ethics Statement

The Khula South Africa birth cohort study received ethical approval from the University of Cape Town Human Ethics Research Committee (HREC; 666/2021; 782/2022). All mothers provided written informed consent for cohort participation at Khula enrolment and for their children to participate in study-specific procedures across timepoints. Given the longitudinal nature of the cohort, study consent is obtained from mothers annually for this cohort.

Conflicts of Interest

The authors declare no conflicts of interest.

Data Availability Statement

Data used for these analyses have been deposited in *ZivaHub Open*, a public repository. This information can be found at the following DOI: https://doi.org/10.25375/uct.29197649.v1.

References

Abate, F., A. Adu-Amankwah, K. Ae-Ngibise, et al. 2024. "UNITY: A Low-Field Magnetic Resonance Neuroimaging Initiative to Characterize Neurodevelopment in Low and Middle-Income Settings." *Developmental Cognitive Neuroscience* 69: 101397.

Anazodo, U. C., J. J. Ng, B. Ehiogu, et al. 2023. "A Framework for Advancing Sustainable Magnetic Resonance Imaging Access in Africa." *NMR in Biomedicine* 36, no. 3: e4846.

Aquino, D., A. Bizzi, M. Grisoli, et al. 2009. "Age-Related Iron Deposition in the Basal Ganglia: Quantitative Analysis in Healthy Subjects." *Radiology* 252, no. 1: 165–172.

Avants, B. B., N. J. Tustison, G. Song, P. A. Cook, A. Klein, and J. C. Gee. 2011. "A Reproducible Evaluation of ANTs Similarity Metric Performance in Brain Image Registration." *NeuroImage* 54, no. 3: 2033–2044.

Avants, B. B., N. J. Tustison, J. Wu, P. A. Cook, and J. C. Gee. 2011. "An Open Source Multivariate Framework for n-Tissue Segmentation With Evaluation on Public Data." *Neuroinformatics* 9: 381–400.

Azhari, A., A. Truzzi, M. J.-Y. Neoh, et al. 2020. "A Decade of Infant Neuroimaging Research: What Have We Learned and Where Are We Going?" *Infant Behavior and Development* 58: 101389.

Baljer, L., U. Briski, R. Leech, et al. 2025. "GAMBAS: Generalised-Hilbert Mamba for Super-Resolution of Paediatric Ultra-Low-Field MRI," Preprint, arXiv. Accessed December 18, 2025. https://doi.org/10.48550/arXiv.2504.04523.

Baljer, L., Y. Zhang, N. J. Bourke, et al. 2025. "Ultra-Low-Field Paediatric MRI in Low-and Middle-Income Countries: Super-Resolution Using a Multi-Orientation U-Net." *Human Brain Mapping* 46, no. 1: e70112.

Barkovich, A. J., and B. Kjos. 1988. "Normal Postnatal Development of the Corpus Callosum as Demonstrated by MR Imaging." *American Journal of Neuroradiology* 9, no. 3: 487–491.

Barkovich, M. J., Y. Li, R. S. Desikan, A. J. Barkovich, and D. Xu. 2019. "Challenges in Pediatric Neuroimaging." *NeuroImage* 185: 793–801.

Basu, S., D. Kumar, S. Anupurba, A. Verma, and A. Kumar. 2018. "Effect of Maternal Iron Deficiency Anemia on Fetal Neural Development." *Journal of Perinatology* 38, no. 3: 233–239.

Casella, C., A. Leknes, N. Bourke, et al. 2025. MiniMORPH: A Morphometry Pipeline for Low-Field MRI in Infants. Preprint, medRxiv. Accessed December 18, 2025. https://doi.org/10.1101/2025.07.01.25330469.

Cawley, P., F. Padormo, D. Cromb, et al. 2023. "Development of Neonatal-Specific Sequences for Portable Ultralow Field Magnetic Resonance Brain Imaging: A Prospective, Single-Centre, Cohort Study." *EClinicalMedicine* 65: 102253.

Chen, L., Z. Wu, D. Hu, et al. 2022. "A 4D Infant Brain Volumetric Atlas Based on the UNC/UMN Baby Connectome Project (BCP) Cohort." *NeuroImage* 253: 119097.

Cover, G., W. G. Herrera, M. P. Bento, S. Appenzeller, and L. Rittner. 2018. "Computational Methods for Corpus Callosum Segmentation on MRI: A Systematic Literature Review." *Computer Methods and Programs in Biomedicine* 154: 25–35.

Croteau-Chonka, E. C., I. I. I. D. C. Dean, J. Remer, H. Dirks, J. O'Muircheartaigh, and S. C. Deoni. 2016. "Examining the Relationships Between Cortical Maturation and White Matter Myelination Throughout Early Childhood." *NeuroImage* 125: 413–421.

Cusick, S. E., and M. K. Georgieff. 2016. "The Role of Nutrition in Brain Development: The Golden Opportunity of the "First 1000 Days"." *Journal of Pediatrics* 175: 16–21.

Dagia, C., and M. Ditchfield. 2008. "3T MRI in Paediatrics: Challenges and Clinical Applications." *European Journal of Radiology* 68, no. 2: 309–319.

Deoni, S., M. M. Bruchhage, J. Beauchemin, et al. 2021. "Accessible Pediatric Neuroimaging Using a Low Field Strength MRI Scanner." *NeuroImage* 238: 118273.

Deoni, S. C., I. I. I. D. C. Dean, J. Remer, H. Dirks, and J. O'Muircheartaigh. 2015. "Cortical Maturation and Myelination in Healthy Toddlers and Young Children." *NeuroImage* 115: 147–161.

Deoni, S. C., P. Medeiros, A. T. Deoni, et al. 2022. "Development of a Mobile Low-Field MRI Scanner." *Scientific Reports* 12, no. 1: 1–9.

Deoni, S. C., E. Mercure, A. Blasi, et al. 2011. "Mapping Infant Brain Myelination With Magnetic Resonance Imaging." *Journal of Neuroscience* 31, no. 2: 784–791.

Deoni, S. C., J. O'Muircheartaigh, E. Ljungberg, M. Huentelman, and S. C. Williams. 2022. "Simultaneous High-Resolution T2-Weighted Imaging and Quantitative T 2 Mapping at Low Magnetic Field Strengths Using a Multiple TE and Multi-Orientation Acquisition Approach." *Magnetic Resonance in Medicine* 88, no. 3: 1273–1281.

Despotović, I., B. Goossens, and W. Philips. 2015. "MRI Segmentation of the Human Brain: Challenges, Methods, and Applications." *Computational and Mathematical Methods in Medicine* 2015, no. 1: 450341.

Donald, K. A., C. J. Wedderburn, W. Barnett, et al. 2019. "Risk and Protective Factors for Child Development: An Observational South African Birth Cohort." *PLoS Medicine* 16, no. 9: e1002920.

Feng, L., H. Li, K. Oishi, et al. 2019. "Age-Specific Gray and White Matter DTI Atlas for Human Brain at 33, 36 and 39 Postmenstrual Weeks." *NeuroImage* 185: 685–698.

Fischl, B., D. H. Salat, E. Busa, et al. 2002. "Whole Brain Segmentation: Automated Labeling of Neuroanatomical Structures in the Human Brain." *Neuron* 33: 341–355.

Georgieff, M. K. 2020. "Iron Deficiency in Pregnancy." *American Journal of Obstetrics and Gynecology* 223: 516–524.

Georgieff, M. K., S. E. Ramel, and S. E. Cusick. 2018. "Nutritional Influences on Brain Development." *Acta Paediatrica* 107, no. 8: 1310–1321.

Gilmore, J. H., F. Shi, S. L. Woolson, et al. 2012. "Longitudinal Development of Cortical and Subcortical Gray Matter From Birth to 2 Years." *Cerebral Cortex* 22, no. 11: 2478–2485.

Hyperfine. 2025. "Portable MR Imaging: Bringing MRI to the Patient." Accessed December 18, 2025. https://hyperfine.io.

IAEA. 2025. "IMAGINE—IAEA Medical imAGIng and Nuclear mEdicine Global Resources Database: MRI Units (Per 1 Mil)." International Atomic Energy Association (IAEA) Human Health Campus. Accessed December 18, 2025. https://humanhealth.iaea.org/HHW/DBStatistics/IMAGINEMaps3.html.

Janbek, J., M. Sarki, I. O. Specht, and B. L. Heitmann. 2019. "A Systematic Literature Review of the Relation Between Iron Status/Anemia in Pregnancy and Offspring Neurodevelopment." *European Journal of Clinical Nutrition* 73, no. 12: 1561–1578.

Knickmeyer, R. C., S. Gouttard, C. Kang, et al. 2008. "A Structural MRI Study of Human Brain Development From Birth to 2 Years." *Journal of Neuroscience* 28, no. 47: 12176–12182.

Loureiro, B., M. Martinez-Biarge, F. Foti, M. Papadaki, F. M. Cowan, and C. J. Wusthoff. 2017. "MRI Patterns of Brain Injury and Neurodevelopmental Outcomes in Neonates With Severe Anaemia at Birth." *Early Human Development* 105: 17–22.

Monk, C., M. K. Georgieff, D. Xu, et al. 2016. "Maternal Prenatal Iron Status and Tissue Organization in the Neonatal Brain." *Pediatric Research* 79, no. 3: 482–488.

Murali, S., H. Ding, F. Adedeji, et al. 2023. "Bringing MRI to Low- and Middle-Income Countries: Directions, Challenges and Potential Solutions." *NMR in Biomedicine* 37: e4992.

Péran, P., A. Cherubini, G. Luccichenti, et al. 2009. "Volume and Iron Content in Basal Ganglia and Thalamus." *Human Brain Mapping* 30, no. 8: 2667–2675.

Quezada-Pinedo, H. G., F. Cassel, L. Duijts, et al. 2021. "Maternal Iron Status in Pregnancy and Child Health Outcomes After Birth: A Systematic Review and Meta-Analysis." *Nutrients* 13, no. 7: 2221.

Ringshaw, J. E., C. J. Hendrikse, C. J. Wedderburn, et al. 2025. "Persistent Impact of Antenatal Maternal Anaemia on Child Brain Structure at 6–7 Years of Age: A South African Child Health Study." *BMC Medicine* 23: 94.

Ringshaw, J. E., S. H. Joshi, and K. A. Donald. 2021a. "Neuroimaging Explainer Video for Toddlers." Cape Universities Body Imaging Centre, University of Cape Town Cape Town, South Africa ScreenPoint Digital. https://cubic.uct.ac.za/resources-tools-researchers/neuroimaging-explainer-videos.

Ringshaw, J. E., S. H. Joshi, and K. A. Donald. 2021b. "Neuroimaging Explainer Video for Children." Cape Universities Body Imaging Centre, University of Cape Town, Cape Town, South Africa: ScreenPoint Digital. https://cubic.uct.ac.za/resources-tools-researchers/neuroimaging-children.

Ringshaw, J. E., C. J. Wedderburn, L. E. Bradford, et al. 2025. "Brain Imaging With Babies: An Explainer Video for Mothers and Caregivers." Cape Universities Body Imaging Centre, University of Cape Town, Cape Town, South Africa: ScreenPoint Digital. https://cubic.uct.ac.za/neuroimaging-children-hyperfine.

Ringshaw, J. E., M. R. Zieff, S. Williams, et al. 2025. "Iron Deficiency Anaemia in Mothers and Infants With High Inflammatory Burden: Prevalence and Profile in a South African Birth Cohort." *PLOS Global Public Health* 5, no. 7: e0004174.

Shi, F., Y. Fan, S. Tang, J. H. Gilmore, W. Lin, and D. Shen. 2010. "Neonatal Brain Image Segmentation in Longitudinal MRI Studies." *NeuroImage* 49, no. 1: 391–400.

Stevens, G. A., C. J. Paciorek, M. C. Flores-Urrutia, et al. 2022. "National, Regional, and Global Estimates of Anaemia by Severity in Women and Children for 2000–19: A Pooled Analysis of Population-Representative Data." *Lancet Global Health* 10, no. 5: e627–e639.

Tanaka-Arakawa, M. M., M. Matsui, C. Tanaka, et al. 2015. "Developmental Changes in the Corpus Callosum From Infancy to Early Adulthood: A Structural Magnetic Resonance Imaging Study." *PLoS One* 10, no. 3: e0118760.

Váša, F., C. Bennallick, N. J. Bourke, et al. 2025. "Ultra-Low-Field Brain MRI Morphometry: Test-Retest Reliability and Correspondence to High-Field MRI." *Imaging Neuroscience* 3: IMAG-a.930.

Wedderburn, C. J., J. E. Ringshaw, K. A. Donald, et al. 2022. "Association of Maternal and Child Anemia With Brain Structure in Early Life in South Africa." *JAMA Network Open* 5, no. 12: e2244772-e.

Wedderburn, C. J., S. Subramoney, S. Yeung, et al. 2020. "Neuroimaging Young Children and Associations With Neurocognitive Development in a South African Birth Cohort Study." *NeuroImage* 219: 116846.

WHO. 2023. Accelerating Anaemia Reduction: A Comprehensive Framework for Action. Accessed December 18, 2025. https://www.who.int/publications/i/item/9789240074033.

Zieff, M. R., M. Miles, E. Mbale, et al. 2024. "Characterizing Developing Executive Functions in the First 1000 Days in South Africa and Malawi: The Khula Study." *Wellcome Open Research* 9, no. 157: 157.